

# Spectral function of the electron in a superconducting RVB state

V.N. Muthukumar,<sup>a</sup> Z.Y. Weng,<sup>b,c</sup> D.N. Sheng<sup>d</sup>

<sup>a</sup> Department of Physics, Princeton University, Princeton, NJ 08544

<sup>b</sup> Center for Advanced Study, Tsinghua University, Beijing 100084

<sup>c</sup> Texas Center for Superconductivity, University of Houston, Houston, TX 77204

<sup>d</sup> Department of Physics and Astronomy, California State University, Northridge, CA 91330

We present a model calculation of the spectral function of an electron in a superconducting resonating valence bond (RVB) state. The RVB state, described by the phase-string mean field theory, is characterized by three important features: (i) spin-charge separation, (ii) short range antiferromagnetic correlations, and (iii) holon condensation. The results of our calculation are in good agreement with data obtained from Angle Resolved Photoemission Spectroscopy (ARPES) in superconducting  $\text{Bi}_2\text{Sr}_2\text{CaCu}_2\text{O}_{8+\delta}$  at optimal doping concentration.

The spectral function of an electron,  $A(\mathbf{k}, \omega)$ , being the probability of finding an electron with momentum  $\mathbf{k}$  and energy  $\omega$ , is a fundamental quantity in any description of interacting electrons. ARPES is a very powerful and direct experimental technique used to measure the spectral function in electronic systems. In the last decade, ARPES measurements have contributed much to our understanding of the high temperature superconductors (HTSC). Measurements done in the normal and the superconducting state of the HTSC reveal a variety of interesting features [1], [2]. For instance, the normal state spectra are extremely broad, with the broad peak evolving into a hump at  $T_c$ . In addition to the hump, a very sharp peak appears below  $T_c$  at low binding energies. This is observed most clearly near the Brillouin zone boundary around the  $M$  points,  $(0, \pm\pi)$  and  $(\pm\pi, 0)$  [3]. The strength of the sharp peak appearing below  $T_c$  is proportional to the superfluid density [4], [5]. Along the direction  $(0, 0) \rightarrow (\pi, \pi)$ , there is some debate if the data below  $T_c$  can be interpreted as showing a clear break between a coherent quasiparticle part and the broad incoherent background [6], [1].

It was first noted by Anderson that spin-charge separation may provide a natural explanation for the ARPES results [7]. The basic idea is that the hole created by a photon decays into a spinless holon and a neutral spinon excitation. Such a decomposition can explain the broad incoherent background seen in photoemission spectra, as well as the absence of a sharp quasiparticle peak in the normal state. The emergence of a sharp quasiparticle state below  $T_c$  is attributed to the condensation of holons. However, as we shall demonstrate in this paper, the inclusion of short range antiferromagnetic (AF) correlations induced by the photohole is crucial to the understanding of the ARPES results. This has been pointed out in the context of photoemission from a Mott insulator [8]. In

this Letter, we consider the photoemission spectra observed in the superconducting state of optimally doped  $\text{Bi}_2\text{Sr}_2\text{CaCu}_2\text{O}_{8+\delta}$  (Bi 2212). We present a model calculation of the spectral function in a superconducting RVB state, incorporating three important features: (i) short range AF correlations, (ii) spin-charge separation, and (iii) holon condensation. We show that such a description provides a consistent explanation for many of the generic features observed in the superconducting state of optimally doped Bi 2212.

*AF oscillations:* We begin with the decomposition of the electron operator in the so-called phase string formulation,  $c_{i\sigma} = h_i^\dagger a_{i\sigma}$ , where  $h_i^\dagger$  is the bosonic holon creation operator, and  $a_{i\sigma}$  is a *composite* spinon operator that satisfies fermionic anticommutation relations [9]. Unlike the conventional slave-boson formalism, the (composite) spinon operator  $a$  is defined by  $a_{i\sigma} \equiv b_{i\sigma} e^{i\hat{\Theta}_{i\sigma}}$ , where  $b_{i\sigma}$  is the bosonic *elementary* spinon annihilation operator and  $\hat{\Theta}_{i\sigma}$ , a nonlocal phase string operator whose origin lies in the fact that a hole moving through a locally AF background always picks up a string of sequential  $\pm$  signs [9]. The factor  $\hat{\Theta}_{i\sigma}$  imposes anticommutation rules on  $a_{i\sigma}$  as well as  $c_{i\sigma}$ .

In the superconducting phase, the holons ( $h_i^\dagger$ ) condense. An elementary nodal (d-wave) fermionic excitation emerges in the spinon sector and its creation operator  $\gamma_{\mathbf{k}\sigma}^\dagger$  is related to the  $a$ -operator, to leading order as [10]  $a_{\mathbf{k}\sigma} |\Psi_G\rangle \propto -\sigma v_{\mathbf{k}} \gamma_{\mathbf{k}\sigma}^\dagger |\Psi_G\rangle$ , where  $v_{\mathbf{k}}$  is defined in the usual manner as  $v_{\mathbf{k}} = \text{sgn}(\Delta_{\mathbf{k}})(1 - \xi_{\mathbf{k}}/E_{\mathbf{k}})^{1/2}/\sqrt{2}$ , with  $E_{\mathbf{k}}^s = \sqrt{\xi_{\mathbf{k}}^2 + \Delta_{\mathbf{k}}^2}$  and  $\Delta_{\mathbf{k}} = \Delta_0(\cos k_x a - \cos k_y a)$ . Thus, the superconducting ground state,  $|\Psi_G\rangle$ , in the phase string description looks quite similar to the d-wave mean field state in the slave-boson approach [11]. However, the above considerations (obtained by using equations of motion), miss the local AF structure around a hole that is created. To see this, let us consider a bare hole state created by the  $c$ -operator,  $c_{i\uparrow} |\Psi_G\rangle$  and measure the spin configuration around the hole by evaluating the quantity  $\langle \Psi_G | c_{i\uparrow}^\dagger S_j^z c_{i\uparrow} | \Psi_G \rangle$ . Now,

$$\begin{aligned} \langle \Psi_G | c_{i\uparrow}^\dagger S_j^z c_{i\uparrow} | \Psi_G \rangle &= \langle \Psi_G | b_{i\uparrow}^\dagger \frac{1}{2} \sum_{\alpha} \alpha b_{j\alpha}^\dagger b_{j\alpha} b_{i\uparrow} | \Psi_G \rangle \\ &= -\frac{1}{2} |\langle \Psi_G | b_{i\uparrow}^\dagger b_{j\downarrow}^\dagger | \Psi_G \rangle|^2 + \frac{1}{2} |\langle \Psi_G | b_{i\uparrow}^\dagger b_{j\uparrow}^\dagger | \Psi_G \rangle|^2. \end{aligned} \quad (1)$$

Using the mean field solution [10], we get

$$\langle \Psi_G | b_{i\uparrow}^\dagger b_{j\downarrow}^\dagger | \Psi_G \rangle = [(-1)^{i-j} - 1] \sum_m u_m v_m w_{m\uparrow}^*(i) w_{m\uparrow}(j), \quad (2)$$

and

$$\langle \Psi_G | b_{i\uparrow}^\dagger b_{j\uparrow}^\dagger | \Psi_G \rangle = [(-1)^{i-j} + 1] \sum_m v_m^2 w_{m\uparrow}^*(i) w_{m\uparrow}(j). \quad (3)$$

In the above,  $u_m$  and  $v_m$  are the ‘‘coherence factors’’ of the mean field theory determined self consistently for a given hole concentration  $\delta$ , within a Bogoliubov-de Gennes scheme, and  $w_{m\sigma}$ , a one particle wave function. Equations (2) and (3) are used in (1) to determine the spin density around the hole site. The results are shown in Fig. 1, where we have plotted the spin density as a function of the hole distance along the  $\hat{x}$  axis for hole concentrations  $\delta = 0$ , and  $\delta = 1/7 \simeq 0.14$ . As seen in the figure, the hole is surrounded by AF oscillations in the local spin density. The oscillation is to be expected from (1) and is indicative of local AF correlations. The ground state  $|\Psi_G\rangle$  is a singlet and the presence of  $c_{i\uparrow}|\Psi_G\rangle$  (an up spin hole) is accompanied by a spinon excitation with  $S^z = -1/2$ . Assuming the (up spin) hole to be located on an odd sublattice site, our results show that the (down) spinon is created only on the even sublattice sites. Note the presence of nonvanishing (up) spin density on the odd sublattice sites, which we interpret as overscreening. Thus, the combination of the up spin hole on an odd site and the down (up) spin response on the odd (even) sites represents a spin-polaron with zero net spin.

To account for this effect in determining the spectral function, we adopt the following empirical approach. We write

$$a_{i\uparrow}|\Psi_G\rangle \simeq \sum_j \eta_j(i) \alpha_{j\downarrow}^\dagger |\Psi_G\rangle + \text{higher order terms}, \quad (4)$$

where  $\eta_j(i) \neq 0$  only for  $i$  and  $j$  not belonging to the same sublattice, and  $\alpha_{\mathbf{k}\sigma} \equiv |v_{\mathbf{k}}| \gamma_{\mathbf{k}\sigma}$  (the d-wave sign in  $v_{\mathbf{k}}$  will be absorbed into  $\eta$ ). We only retain the nearest and third nearest neighboring sites in the expansion (4); *viz.*,  $\eta_j(i) = +(-)\eta_0/2$ , if  $j = i \pm \hat{x}(\hat{y})$ ;  $\eta_j(i) = +(-)\eta_1/2$ , if  $j = i \pm 2\hat{x}(\hat{x}) \pm \hat{y}(2\hat{y})$ ;  $\eta_j(i) \approx 0$  for all other sites. The sign of  $\eta_j(i)$  is from the d-wave symmetry of spinon pairing. Transforming to momentum space, we get, within this approximation,  $a_{\mathbf{k}\uparrow}|\Psi_G\rangle \approx \eta_{\mathbf{k}} |v_{\mathbf{k}}| \gamma_{-\mathbf{k}\downarrow}^\dagger |\Psi_G\rangle$ , where

$$\eta_{\mathbf{k}} = \eta_0 (\cos k_x a - \cos k_y a) + 2\eta_1 (\cos k_x a \cos 2k_y a - \cos k_y a \cos 2k_x a). \quad (5)$$

Here we take  $\eta_1/\eta_0 \simeq 0.3$  for  $\delta = 0.14$ .

We may now ask what happens when an electron is created (as, for example, in inverse photoemission), *i.e.*,  $c_{i\uparrow}^\dagger |\Psi_G\rangle$ . It can be shown in this case that the  $\uparrow$  spinon

is created at the site  $i$  with some residual amplitude extended over other sites of the same sublattice. Neglecting the residual amplitude, to leading order we get

$$a_{\mathbf{k}\uparrow}^\dagger |\Psi_G\rangle \simeq u_{\mathbf{k}} \gamma_{\mathbf{k}\uparrow}^\dagger |\Psi_G\rangle,$$

which is essentially the same as the slave-boson result. In the above,  $u_{\mathbf{k}}^2 = 1 - v_{\mathbf{k}}^2$ . Therefore, the main distinction between the usual d-wave slave-boson mean field theory and this calculation is the momentum dependent factor  $\eta_{\mathbf{k}}$  that arises in the hole channel (corresponding to the creation of a photohole in ARPES). The remainder of this paper is devoted to a study of this channel. The differences between particle and hole spectroscopies as well as a detailed comparison with slave-boson theories will be presented elsewhere.

*Spin-charge separation and holon condensation:* In the superconducting state, the spinons are paired with d-wave symmetry as discussed earlier. The effective hamiltonian for the holons is given by  $H_h = -t_h \sum_{\langle ij \rangle} e^{iA_{ij}^f} h_i^\dagger h_j + \text{h.c.}$ , where  $A_{ij}^f$  represents the gauge field due to the spinons seen by the holons. Since the spinons are paired, the mean field solution leads to the result  $\sum_{\square} A_{ij}^f \approx -\pi$  [10]. Thus the superconducting state is described by paired spinons and a Bose condensate of holons that experience a  $\pi$  flux around an elementary plaquette. Based on our earlier discussion, we obtain the spectral function of the spinons,  $\rho_a(\mathbf{k}, \omega) = \eta_{\mathbf{k}}^2 v_{\mathbf{k}}^2 \delta(\omega + E_{\mathbf{k}}^s)$ . The spectral function for the holons is easily derived as

$$\rho_h(\mathbf{k}, \omega) = \cos^2 \frac{\theta_{\mathbf{k}}}{2} \delta(\omega - \epsilon_{\mathbf{k}-}^h) + \sin^2 \frac{\theta_{\mathbf{k}}}{2} \delta(\omega - \epsilon_{\mathbf{k}+}^h),$$

where  $\cos \theta_{\mathbf{k}} = \gamma_{\mathbf{k}} / (\sqrt{2} \lambda_{\mathbf{k}})$ . Here,  $\gamma_{\mathbf{k}} = \cos k_x a + \cos k_y a$ ,  $\lambda_{\mathbf{k}} = \sqrt{\cos^2 k_x a + \cos^2 k_y a}$ , and  $\epsilon_{\mathbf{k}\pm}^h = \pm 2t_h \lambda_{\mathbf{k}} - \mu_h$ . At  $T = 0$ , the holon chemical potential  $\mu_h = -2t_h \lambda_{\mathbf{k}=0} = -2\sqrt{2}t_h$ .

We now construct the spectral function of the electron by using the operator decomposition of the electron,  $c_{i\sigma} = h_0 a_{i\sigma} + c'_{i\sigma}$ , where  $\langle h_i^\dagger \rangle = h_0$ , describes the Bose condensate of holons, and  $c'_{i\sigma} =: h_i^\dagger : a_{i\sigma}$ , with  $: h_i^\dagger := h_i^\dagger - h_0$ . The spectral function of the electron  $A_-^e(\mathbf{k}, \omega)$ , is expressed as a convolution of the spinon and holon spectral functions. It is easy to see that

$$A_-^e(\mathbf{k}, \omega) = \theta(-\omega) \frac{1}{N} \sum_{\mathbf{k}} \int_{\omega}^0 d\omega' \rho_h(\mathbf{k}' - \mathbf{k}, \omega' - \omega) \rho_a(\mathbf{k}', \omega), \quad (6)$$

where  $\rho_a$  and  $\rho_h$  are the spectral functions of the spinon and holon respectively. For obvious reasons, we write the spectral function as the sum of an incoherent and a coherent part,  $A_-^e = A_-^i + A_-^c$ . Clearly, these two terms correspond to the two terms in the electron decomposition.

The coherent part of the spectral function is obtained from the contribution of the holon condensate. We get

$$A_-^c(\mathbf{k}, \omega) = \rho_h^c \eta_{\mathbf{k}}^2 v_{\mathbf{k}}^2 \delta(\omega + E_{\mathbf{k}}^s), \quad (7)$$

where  $\rho_h^c \propto \delta$  denotes the density of the holon condensate. This contribution is dubbed “coherent”, since it is a sharp peak appearing below  $T_c$  (the temperature at which the holons condense). The incoherent part of the spectral function is the convolution,

$$A_-^i(\mathbf{k}, \omega) = \frac{1}{N} \sum_{\mathbf{k}'} \eta_{\mathbf{k}'+\mathbf{k}}^2 v_{\mathbf{k}'+\mathbf{k}}^2 [\cos^2 \frac{\theta_{\mathbf{k}}}{2} \delta(\omega + E_{\mathbf{k}'+\mathbf{k}}^s + \epsilon_{\mathbf{k}'-}^h) + \sin^2 \frac{\theta_{\mathbf{k}}}{2} \delta(\omega + E_{\mathbf{k}'+\mathbf{k}}^s + \epsilon_{\mathbf{k}'+}^h)]. \quad (8)$$

The prime in the summation indicates that the contribution from the holon condensate is removed.

*Comparison with ARPES results:* We are now in a position to plot  $A_-^e(\mathbf{k}, \omega)$  for various momenta and compare with results from ARPES. For the calculation of the spectral function, we choose the following parameters. The dispersion of the spinons,  $\xi_{\mathbf{k}}$ , is determined by the nearest and next nearest neighbor hopping integrals,  $t_1 = 75$  meV,  $t_2 = 20$  meV. The chemical potential,  $\mu = -62$  meV is chosen to mimic the topography of the observed Fermi surface. We choose a value of  $\Delta = 20$  meV for the gap, and  $t_h = 4t_1 = 0.3$  eV for the holon dispersion. Before proceeding to discuss the results for  $A_-^e(\mathbf{k}, \omega)$ , we note that the following can be anticipated: (a) The coherent part of the spectral function,  $A_-^c(\mathbf{k}, \omega) \propto \rho_h^c \propto \delta$ . So, the strength of the coherent peak will be proportional to the superfluid density, as observed experimentally [5], [4]. (b) As is evident from our results,  $A_-^c(\mathbf{k}, \omega)$  is *strongly* momentum dependent, owing to the factor  $\eta_{\mathbf{k}}^2$ . This contribution is strongest around the  $M$  point and weakest around the  $\Gamma$  point. (c) The incoherent part of the spectral function is expected to produce a broad background. Such a broad background is always seen in photoemission. Since, in our calculation, the background arises from a convolution of spinon and holon spectral functions, we expect a rather *weak* momentum dependence of the broad background. This may have already been observed experimentally [12].

In Fig. 2, we show the results for  $A_-^e(\mathbf{k}, \omega)$  at a point on the Fermi surface,  $\mathbf{k} = (0.4, \pi)$ . We see clearly that the total spectral response is the sum of the incoherent and coherent pieces of the spectral function. The sharp peak at lower binding energy corresponds to  $A_-^c$  and the peak is located at an energy  $\omega = E_{\mathbf{k}}^s$ . The broad feature seen in the figure is the contribution from  $A_-^i$ . The incoherent part exhibits a low energy edge around  $E_{\mathbf{k}}^s$ , and a broad peak (“hump”) slightly above it. The origin of these features is very much the same as in the spectra of the undoped insulator [8]. In both cases, the low energy edge is determined by the dispersion of the spinon,  $E_{\mathbf{k}}^s$ . The origin of the hump lies in the local AF correlations

embodied in the factor  $\eta_{\mathbf{k}}$ . Let us consider (8). The factor  $\eta_{\mathbf{k}}$  is maximum at the  $M$  point. As  $\omega$  increases,  $\mathbf{k}' \neq 0$  terms in (8) have to contribute to the sum. However, for such terms, the factor  $\eta_{\mathbf{k}+\mathbf{k}'}$  decreases, thereby causing a hump in the spectral function. The position of the hump is shifted from the edge by  $\epsilon_{\mathbf{k}'-}^h$ . A similar effect occurs in the photoemission of a single hole in the Mott insulator, where a broad hump arises from the coherence factors of the Schwinger boson mean field theory. We emphasize that the factor  $\eta_{\mathbf{k}}$  in the present case and the coherence factors in the Schwinger boson theory of the insulator reflect the antiferromagnetic correlations that play an important role in the formation of the observed humps. Seen in this perspective, the hump is not directly related to the 41 meV resonance observed in the neutron scattering [13], as conjectured in the literature [14] though AF correlations clearly play a crucial role in both explanations.

In Fig. 3, we show the behavior of  $A_-^e(\mathbf{k}, \omega)$  for various  $\mathbf{k}$  points. In the left panel, we show how the spectral function evolves as one moves away from the  $M$  point in two perpendicular directions. As can be seen in the figure, the peak-dip-hump structure gets more pronounced near the  $M$  point. In the right panel, we show the spectral function for a series of points on the Fermi surface. Again, we see that the factor  $\eta_{\mathbf{k}}$  causes the coherent peak as well as the hump to diminish away from the  $M$  point. In particular, along the direction  $\Gamma \rightarrow (\pi, \pi)$ , these features are absent in our calculation. Though this is an approximate result, it shows that the inclusion of AF correlations suppresses the peak-dip-hump structure along this direction.

To conclude, our model calculation of the spectral function of an electron in a superconducting RVB state explains many of the generic features observed in the photoemission spectra of optimally doped Bi 2212. We find that the inclusion of short range antiferromagnetic correlations is extremely crucial to the understanding of these features. In particular, we show that the presence of a hole induces Friedel-like oscillations in the local spin density surrounding the hole. We propose a scheme to incorporate this effect in the calculation of the spectral function. When this is taken into account in conjunction with spin-charge separation and holon condensation below superconducting  $T_c$ , many of the features seen in photoemission can be explained naturally. Our calculation shows that these features have analogues in the photoemission spectra of the undoped Mott insulator where the short range antiferromagnetic correlations play a very important role too.

We thank P. W. Anderson for his comments. We are also thankful to H. Ding, A. Fedorov, P. D. Johnson, T. Valla and B. O. Wells for several discussions on ARPES. V.N.M. is supported by NSF Grant DMR-9104873. V.N.M. also thanks the hospitality at Texas Center for Superconductivity, University of Houston

where part of this work was carried out.

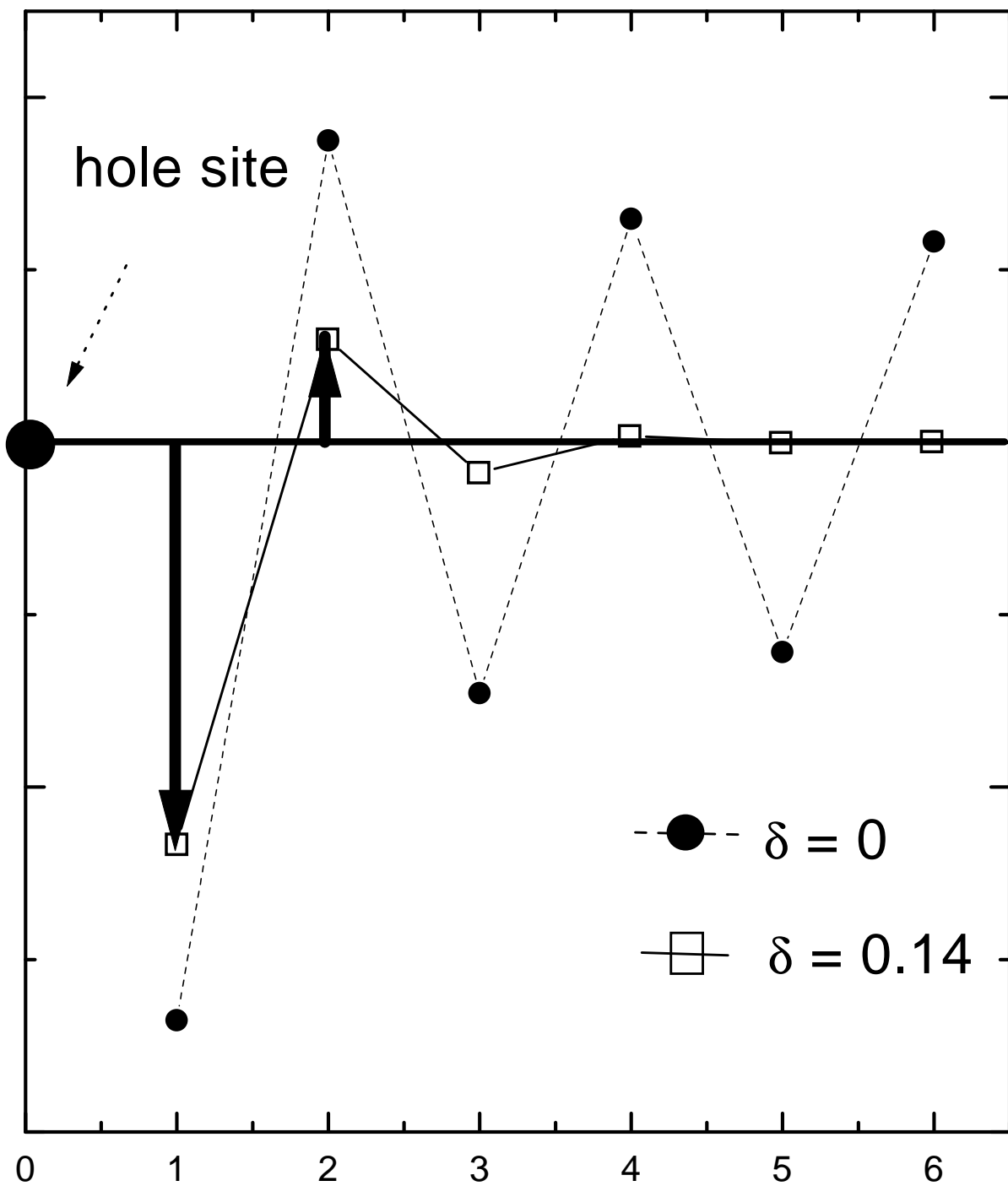
---

- [1] For a recent review, see, J. C. Campuzano in *More is Different*, Princeton Series in Physics (Princeton University Press, Princeton, 2001).
- [2] Takami Tohyama and Sadamichi Maekawa, *Supercond. Sci. Technol.* **13**, R17 (2000).
- [3] A. V. Fedorov *et al.*, *Phys. Rev. Lett.* **82**, 2179 (1999).
- [4] D. L. Feng *et al.*, *Science* **289**, 277 (2000).
- [5] H. Ding *et al.*, cond-mat/0006143.
- [6] T. Valla *et al.*, *Science* **285**, 2110 (1999).
- [7] P. W. Anderson, *The Theory of Superconductivity in the High  $T_c$  Cuprates* (Princeton University Press, Princeton, 1997).
- [8] Z. Y. Weng, V. N. Muthukumar, D. N. Sheng and C. S. Ting, *Phys. Rev. B* **63**, 075102 (2001).
- [9] Z. Y. Weng, D. N. Sheng, Y.-C. Chen, and C. S. Ting, *Phys. Rev. B* **55**, 3894 (1997).
- [10] Z. Y. Weng, D. N. Sheng, and C. S. Ting, *Phys. Rev. B* **61**, 12328 (2000).
- [11] P.A. Lee and N. Nagaosa, *Phys. Rev. B* **46**, 5621 (1992); X.G. Wen and P.A. Lee, *Phys. Rev. Lett.* **76**, 503 (1996); Jian-Xin Li, Chung-Yu Mou, and T. K. Lee, *Phys. Rev. B* **62**, 640 (2000); C. Lannert, M.P.A. Fisher, and T. Senthil, cond-mat/0101249.
- [12] T. Valla *et al.*, unpublished.
- [13] H.F. Hong *et al.* *Phys. Rev. Lett.* **75**, 316 (1995).
- [14] J.C. Campuzano, *Phys. Rev. Lett.* **83**, 3709 (1999).

Fig. 1 Spin configuration near an up-spin hole, created by  $c_{\uparrow}$  on the ground state at  $\delta = 0$  and 0.14, along the  $\hat{x}$  axis.

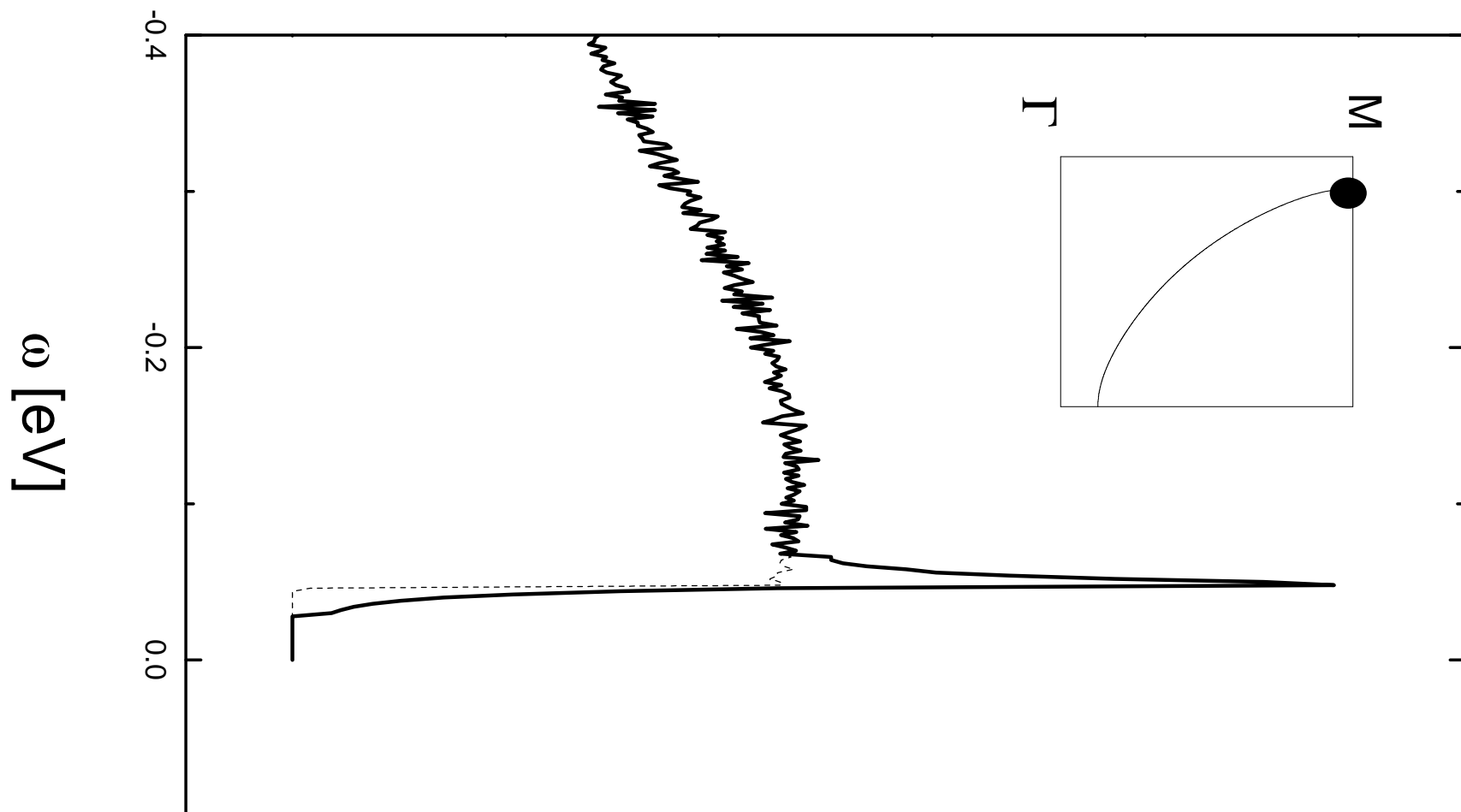
Fig. 2 The spectral function at  $\mathbf{k}=(0.4, \pi)$ , which is a Fermi point at the Brillouin zone boundary (see the inset). The dashed curve shows only the incoherent part whose low energy edge coincides with the coherent peak position while its ‘hump’ lies slightly above the edge.

Fig.3 The spectral function at different momenta marked by full circles in the insets of two panels. The left panel corresponds to scans near the M point along two directions, while the right represents momenta on the Fermi surface.

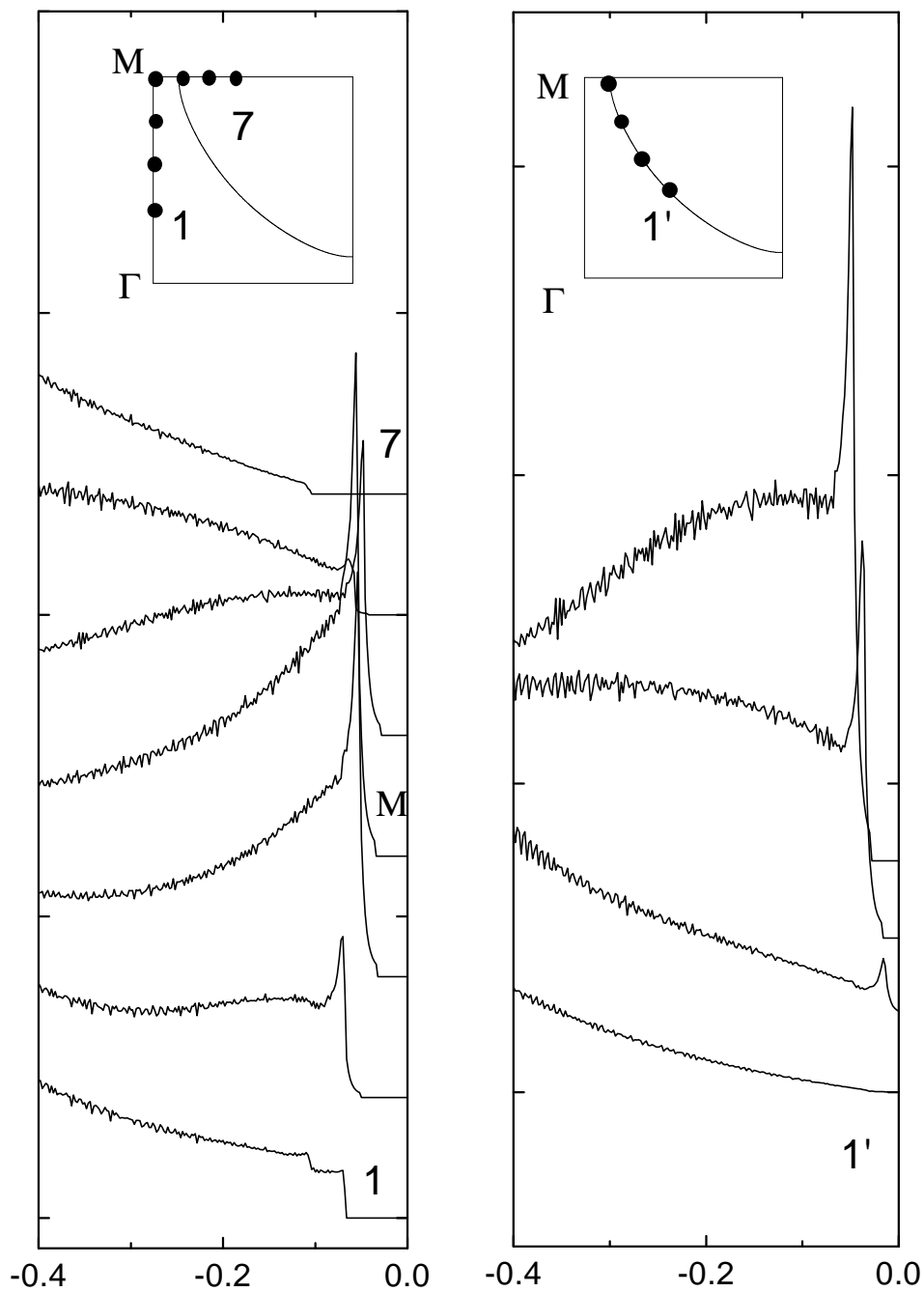


Distance from the hole along x-axis

# Spectral function (arb. units)



Spectral function (arb. units)



$\omega$  [eV]